Carbohydrate Polymers 105 (2014) 10–19

Contents lists available at ScienceDirect

Carbohydrate Polymers

journal homepage: www.elsevier.com/locate/carbpol

Physical properties of inulin and inulin–orange juice: Physical characterization and technological application

M.Z. Saavedra-Leos[a], C. Leyva-Porras[c,d], E. Martínez-Guerra[c], S.A. Pérez-García[c], J.A. Aguilar-Martínez[c], C. Álvarez-Salas[b,*]

[a] Coordinación Académica Región Altiplano, Universidad Autónoma de San Luis Potosí, Carretera Cedral Km. 5+600, Ejido San José de las Trojes, Matehuala C.P. 78700, S.L.P., Mexico
[b] Facultad de Ingeniería, Universidad Autónoma de San Luis Potosí, Av. Dr. Manuel Nava No. 6, Zona Universitaria, San Luis Potosí C.P. 78210, S.L.P., Mexico
[c] Centro de Investigación en Materiales Avanzados S.C. (CIMAV), Alianza Norte No. 202, Autopista Monterrey-Aeropuerto Km 10, Parque de Investigación e Innovación Tecnológica (PIIT), Apodaca C.P. 66600, N.L., Mexico
[d] Centro de Investigación en Materiales DIP-CUCEI, Universidad de Guadalajara, Av. Revolución # 1500, Col. Olímpica, Guadalajara C.P. 44430, Jal, Mexico

ARTICLE INFO

Article history:
Received 9 September 2013
Received in revised form
16 December 2013
Accepted 28 December 2013
Available online 7 January 2014

Keywords:
Inulin–orange juice system
Water activity
Glass transition temperature
Physical stability
Food products

ABSTRACT

In this work two systems based on a carbohydrate polymer were studied: inulin as model system and inulin–orange juice as complex system. Both system were stored at different water activity conditions and subsequently characterized. Water adsorption isotherms type II were fitted by the GAB model and the water monolayer content was determined for each system. From thermal analyzes it was found that at low water activities (a_w) systems were fully amorphous. As a_w increased, crystallinity was developed. This behavior was corroborated by X-ray diffraction. In the inulin–orange juice system, crystallization appears at lower water activity caused by the intensification of the chemical interaction of the low molecular weight species contained in orange juice. Glass transition temperature (T_g), determined by modulated differential scanning calorimeter, decreased with a_w. As water is adsorbed, the physical appearance of samples changed which could be observed by optical microscopy and effectively related with the microstructure found by scanning electron microscopy.

1. Introduction

Inulin is a storage carbohydrate found in many plants, vegetables, fruits and cereals. The chemical structure is composed by linear chains of fructose molecules joined by β-(2-1) glycosidic bonds terminated by an α-D-(1-2)-glucopyranoside ring group (glucose) (André, Putaux, et al., 1996; André, Mazeau, et al., 1996; Pitarresi, Giacomazza, Triolo, Giammona, & Biagio, 2012). Regularly, linear chains have a length of 3 to 60 units of fructose with molecular weight ranging from 3500 to 5500 Da (Derycke & Vandamme, 1984). Industrially, inulin is extracted from chicory root (*Cichorium intybus*) and is used as an ingredient in foods, contributing to the improvement of the product and providing a beneficial effect for humans (Kawai, Fukami, Thanatuksorn, Viriyarattanasak, & Kajiwara, 2011).

Inulin partially exists in the amorphous state, which can be reached by a rapid change from an equilibrium state into a non-equilibrium state. The non-equilibrium state can be reached by removing the dispersion media i.e. water, or by rapid cooling at temperatures below the melting temperature. Amorphous state is induced in processes as cooling, extrusion and dehydration. Accordingly to Chiou and Langrish (2007), the amorphous state is beneficial in powder products since shelf life is longer. In this state, high viscosity is presented and chemical and biochemical reactions are generally restricted, achieving greater food stability. However, amorphous systems are considered as meta-stable states which are susceptible to undergo crystallization or structural relaxation in order to reach the equilibrium condition. Change velocity between the non-equilibrium and equilibrium states depends on factors such are temperature, time and water content (Roos, 1995; Slade & Levine, 1988). Several studies have been performed with the aim of analyzing the stability of inulin during storage in different fields such as pharmaceutical and food industry (André, Putaux, et al., 1996; André, Mazeau, et al., 1996; Dan, Ghosh, & Moulik, 2009; Glibowski & Pikus, 2011; Kawai et al., 2011; Pitarresi et al., 2012; Ronkart et al., 2006; Ronkart, Paquot, Fougnies, Deroanne, & Blecker, 2009; Zimeri & Kokini, 2003). In these fields, inulin has been employed as an excipient, additive, technological agent, thickener, emulsifier, gelling and sugar substitute. Based on those

* Corresponding author. Tel.: +52 444 8262330x2104; fax: +52 444 8262336.
E-mail addresses: claudia.salas@uaslp.mx, claudia120774@yahoo.com.mx (C. Álvarez-Salas).

0144-8617/$ – see front matter © 2014 Elsevier Ltd. All rights reserved.
http://dx.doi.org/10.1016/j.carbpol.2013.12.079

studies, for an amorphous material such as inulin, the most important parameter affecting the product stability is the glass transition temperature (T_g). T_g is a second order transition defined as the change between the glassy and rubbery states, observed during the variation in temperature and influenced by the water content (Rhaman, 2010; Sablani, Syamaladevi, & Swanson, 2010).

From the physical stability point of view, the most common problems arising during the handling of amorphous powders are: cohesiveness, stickiness and agglomeration, crystallization of sugars, loss of volatile compounds and loss of crunchiness (Adhikari, Howes, Lecomte, & Bhandari, 2001; Khalloufi, El-Maslouhi, & Ratti, 2000; Labuza & Hyman, 1998). Recently, the concepts of water activity (a_w) and glass transition temperature have been used together for evaluating the storage stability of inulin. Results have shown that inulin is more stable when stored at temperature below its T_g and at a_w near the monolayer level. Nevertheless, in most of these studies inulin has been analyzed as a model system. Kawai et al. (2011) studied the effect of water content, molecular weight and crystallinity of inulin on the T_g. Zimeri and Kokini (2003) determined T_g for inulin–water mixtures and inulin with different water contents. Ronkart et al. (2006, 2009) studied the T_g from inulin with polymerization degrees of 10 and 30, respectively. On the other hand, food products deviate from the model systems due to the interactions among the different added ingredients and thus are considered as complex systems.

Therefore, in this work we present the physical characterization of a model and a complex systems, inulin and inulin–orange juice, respectively. The study contributes to a better understanding of the role of the physical properties of the systems in the stability of food products during storage. The proposed methodology is useful in the science and industry fields. For this purpose, dried powders were first saturated with different water contents and representative samples were characterized by thermal analysis, X-ray diffraction, electron microscopy and optical microscopy. Results are discussed in terms of water content, chemical interactions, thermal properties and microstructure.

2. Experimental

2.1. Sample preparation

2.1.1. Spray drying

Crystalline inulin (99.9% purity, Sigma Chemical Co., USA) with melting temperature of 158–165 °C was employed as the starting material for the dehydration process. Orange juice was prepared in the laboratory according to the following composition (w/w): 8.5% of total sugars (53% sucrose, 25.5% fructose and 21.5% glucose), 86.1% of water and 5.4% of other components (proteins, vitamins and minerals) (Arthey & Ashurst, 2001; Farnworth, Lagacé, Couture, Yaylayan, & Stewart, 2001). Two solutions containing inulin–water and inulin–orange juice at a composition of 30–70 w/w were prepared for the spray drying. Dehydration was carried out in a Mini Spray Dryer B290 (Buchi, Switzerland). Sample was fed into the dryer at a temperature of 40 °C, with a volumetric flow of 7 mL/min and a constant pressure of 1.5 bar. Air flow was set at 28 m^3/h, inlet and outlet temperature were recorded as 210 and 70 °C, respectively. For obtaining a fully dried product, inulin and inulin–orange juice samples were placed for seven days into a desiccator containing phosphorous oxide (V) (P_2O_5).

2.1.2. Sorption isotherms

From each dried sample, approximately 2 g were placed into a closed container holding saturated reagents. Different reagents were used for reaching the water saturation equilibrium (a_w): NaOH (0.050), $CaCl_2$ (0.210), K_2CO_3 (0.437), $MgCl_2$ (0.523), $SrCl_2$ (0.710) and KCl (0.834). These reagents were used in order to cover a wider range of water activities. Incubating temperature was chosen based on an average storage temperature, considering the range 25–35 °C. Dried samples were left incubating at 30 °C for 30 days (Kiranoudis, Maroulis, Tsami, & Marinos-Kouris, 1993). After the incubation time elapsed, water activity (a_w) was measured into an Aqualab Series 3 Water Activity Meter (Decagon Devices, Inc. USA). Water content was determined accordingly to the AOAC method, which requires drying the sample in an oven at 110 °C for 2 h.

2.2. Thermal analysis

Thermogravimetric (TGA) and differential scanning calorimetry (DSC) analyses were carried out in a simultaneous TGA-DSC SDT Q600 (TA Instruments, USA). Baseline was calibrated with Indium with a melting temperature of 156.6 °C and melting enthalpy of 28.47 J/g. Samples of 5–10 mg were encapsulated in standard aluminum pans. Thermograms were recorded at a heating rate of 5 °C/min over a range of 25–500 °C. Using the Universal Analysis 2000© software, several features from the curves were identified: mass loss (% w/w), initial ($T_{m\ onset}$), peak ($T_{m\ peak}$) and final ($T_{m\ endset}$) melting temperature, initial ($T_{d\ onset}$), peak ($T_{d\ peak}$) and final ($T_{d\ endset}$) degradation temperature.

2.3. Modulated differential scanning calorimetry (MDSC)

A modulated DSC Q200 (TA Instruments) equipped with an RCS90 cooling system was employed for accurately determining the glass transition temperature (T_g) of the samples. Instrument was also calibrated with Indium for melting temperature and enthalpy, while for heat capacity (C_p) Sapphire was used as the standard. Samples ranging in 5–10 mg were encapsulated in Tzero® aluminum pans. Thermograms were acquired at a temperature range of −90 to 250 °C, with a modulation period of 40 s and amplitude of 1.5 °C. Each experiment was repeated three times.

2.4. Structural analysis by X-ray diffraction (XRD)

The structure of the inulin and inulin–orange juice samples was qualitatively determined by XRD analysis in an X'Pert Empyrean diffractometer (PANalytical, The Netherlands) equipped with Cu-Kα radiation (l = 1.5406 A) operated at 45 kV, 40 mA and a X'Celerator detector in a Bragg-Brentano geometry. Scans were performed in the 2θ range of 10–100°, with step size of 0.016° and 20 s per step.

2.5. Microstructure and optical appearance

2.5.1. Scanning electron microscopy (SEM)

The detailed microstructure of the samples was studied by SEM. Powders from inulin and inulin–orange juice samples were directly deposited onto carbon tape. Images at different magnifications were acquired with a Quanta 200 scanning electron microscope (FEI™, The Netherlands), operated at 15 kV, pressure of 60 Pa and equipped with a backscattered electron detector (BSD).

2.5.2. Optical microscopy

Overall morphology was evaluated by optical microscopy employing a research stereomicroscope SZX16 (Olympus©, USA). Micrographs were acquired at 7X with a digital camera of 1.3 Mpx. Images were analyzed and processed with the software Image Pro Plus version 6.0.

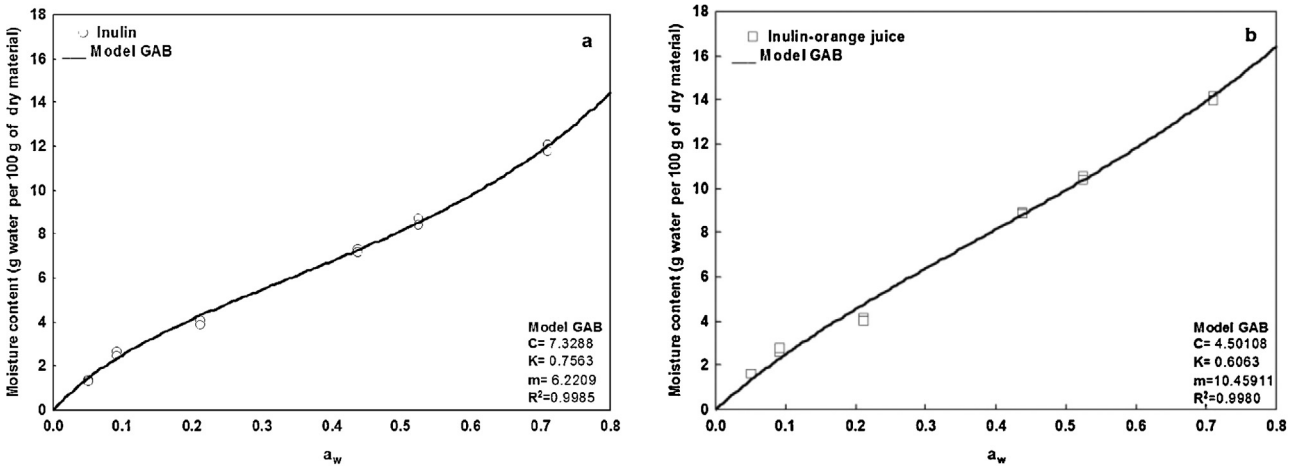

Fig. 1. Moisture adsorption isotherms at 30 °C. (a) Inulin (open circles) and (b) inulin–orange juice (open squares), fitted to the GAB model (solid line).

3. Results and discussion

3.1. Sorption isotherms

Fig. 1 shows the equilibrium moisture content for water activities (a_w) from 0.05–0.710 and for both inulin and inulin–orange juice systems at 30 °C. Equilibrium moisture content is expressed as the amount of water adsorbed (in grams) per 100 g of dried sample. The continuous line joining the scattered points represents the regression according to the GAB model. According to the Brunauer classification (Brunauer, Deming, Deming, & Teller, 1940), the shape of the sigmoid curves corresponds to an isotherm type II. This type of isotherm presents a multilayer adsorption on non-porous solids, with an inflection point at a_w and an asymptotic behavior at high water activities. This adsorption behavior shows that water molecules are selectively adsorbed on certain areas of the sample with higher chemical affinity. This results in an uneven adsorption of water molecules over the surface of the sample, presenting clean zones, zones covered by a single water monolayer and others covered with multilayers. According to the BET and GAB models, the sigmoidal shape of isotherms may be described as an adsorption process in three stages. In zone I (for a_w values from 0 up to 0.25), water molecules are strongly adsorbed on the surface directly interacting with the polar groups presented in the system, forming single water layers. Thus, these single water layers have low molecular mobility, being unable of dissolving the solute and participating in chemical reactions. The boundary between zones I and II is associated to the monolayer water. In zone II, established for a_w values between 0.25–0.80, more water molecules are being added upon the polar group forming multilayers, which are kept on the surface of the solid by capillary condensation. These water multilayers may participate in biochemical reactions and behave as a solvent for low molecular weight solutes. Finally, zone III is presented at a_w values greater than 0.8, where an excess of water molecules are located in the free intermolecular space or forming the liquid phase. This water is available as solvent and for the development of microorganisms. The adsorption isotherms showed that inulin–orange juice samples adsorbed more water than inulin, and this effect is more evident at higher water activities. Inulin–orange juice system presented a water content of 6 g of water per 100 g of dry material in the water activity range of 0.1–0.3, while inulin adsorbed 5 g of water per 100 g of dry material in the same range of a_w. Water sorption in food is a complex phenomenon, which varies with chemical composition, structure and environmental conditions as room temperature (Goula, Karapantsios, Achilias, & Adamopoulos, 2008; Jaya & Das, 2009; Roos, 2002; Sablani, Kasapis, & Rahman, 2007). At a_w higher than 0.5, inulin–orange juice showed higher water adsorption than inulin. This increase in water content is caused by the availability of active sites of crystalline sugars as glucose and fructose. The surface of these sugars presents more OH groups, where water molecules are physically adsorbed. Clearly, this type of curves can be useful in developing new products, as well as in the design and optimization of processes, providing a relationship between water content and the stability during product storage.

Regarding the constants C and k from the GAB model, and according to the analysis performed by Lewicki (1997), if the constant values are within the ranges of $5.67 \leq C \leq \infty$ and $0.24 \leq k \leq 1$, then the predicted monolayer water content will vary between ±15% of its actual value. Then, when comparing the values of the C and k constants for the two systems studied in this work, it is clearly observed that the constants values are between those limits, indicating a good prediction of the monolayer water content.

3.2. Simultaneous thermal analysis (TGA-DSC)

Through simultaneous TGA-DSC experiments, thermograms for the systems inulin and inulin–orange juice were acquired and are presented in Fig. 2. In this figure, two thermograms for each system are shown, each one representing the extreme water activities e.g. 0.05 and 0.710. From the thermograms, different features were identified and these values are summarized in Table 1. At water activity of 0.05 a single endotherm is observed at 230 and 220 °C for the inulin and inulin–orange juice, respectively. This endotherm is associated with a first order transition corresponding to thermal degradation. For inulin, thermal degradation has been reported in the temperature range of 200–250 °C (Dan et al., 2009; Ronkart et al., 2006). We assume that the systems are completely amorphous since the endotherm is accompanied by a large loss weight. In the corresponding TGA, a mass loss of about 30% is observed when temperature increased from $T_{d\ onset}$ to $T_{d\ endset}$. This mass loss is attributed to the decomposition of long molecular chains, polymerization processes and isomerization reactions linked to dehydration (Abd-Elrahman & Ahmed, 2009; Jiang, Liu, Bhandari, & Zhou, 2008; Lee, Thomas & Schnit, 2011; Orsi, 1973; Vanhal & Blond, 1999). At a temperature of 500 °C, both systems showed a final mass loss of 70% corresponding to the full decomposition of the organic matter. In the other hand, at a water activity of 0.710, inulin showed two endotherms at 173 and 230 °C. These were identified as the melting ($T_{m\ peak}$) and degradation ($T_{d\ peak}$) transitions, respectively. At 173 °C the TGA shows a mass loss of about 14%, which corresponds to the water evaporation from the system and

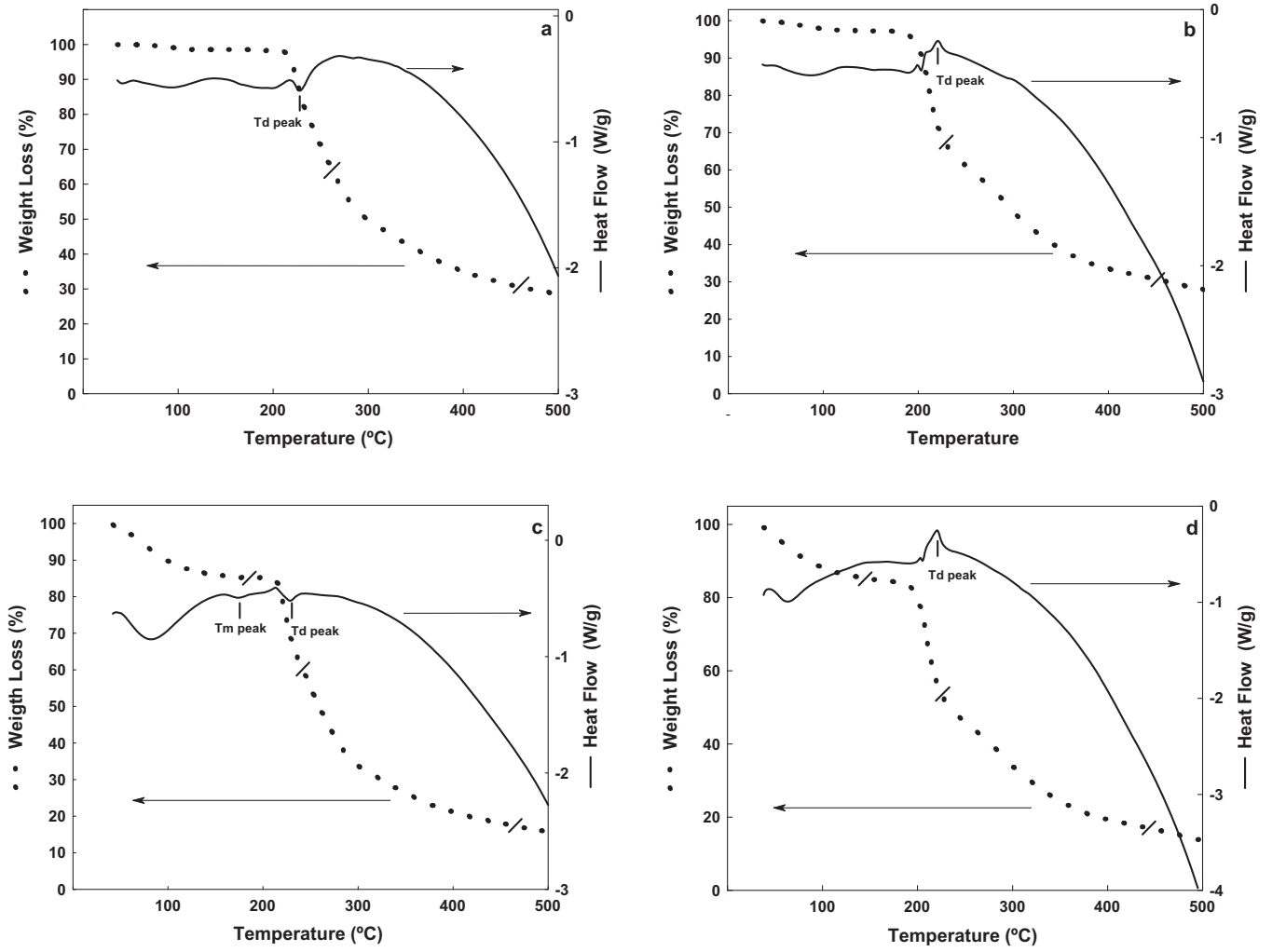

Fig. 2. Simultaneous thermal analysis from the systems at the extreme a_w. TGA is represented by the dotted curve, while DSC is represented by the continuous curve. (a) Inulin at a_w = 0.050, (b) inulin–orange juice at a_w = 0.050, (c) inulin at a_w = 0.710 and (d) inulin–orange juice at a_w = 0.710.

the initial hydrolysis of the polymer chains in inulin. In the range of the degradation temperature from $T_{d\ onset}$ to $T_{d\ endset}$, there is a secondary mass loss, reaching a weight decrease of 70%, related to the decomposition processes aforementioned. Interestingly, at water activity of 0.710 inulin–orange juice system showed again a single endotherm associated to thermal degradation. The melting temperature cannot be observed either because the melting transition is very small or due to the overlapping of the water evaporation in the temperature range of 50–150 °C. From the TGA, an initial mass loss of 18% is observed in the range of 50–200 °C. This corresponds to the degradation of the low molecular weight components in orange juice and to the evaporation of water from the system. Several works from literature have reported that in sugar rich systems, first order transitions such as melting and thermal degradation, take place in a very narrow temperature range (Saavedra-Leos et al., 2012). In the case of low molecular weight sugars, Hurtta, Pitkänen,

Table 1
Thermal characterization results: melting and degradation temperatures of inulin and inulin–orange juice systems at the extreme water activities (a_w = 0.050 and 0.710).

Melting temperature (°C)					
a_w	System	$T_{m\ onset}$	$T_{m\ peak}$	$T_{m\ endset}$	ΔH_m (J/g)
0.050	Inulin	–	–	–	–
	Inulin–orange juice	–	–	–	–
0.710	Inulin	167.64 ± 0.25	173.18 ± 1.46	190.29 ± 4.7	5.87 ± 3.91
	Inulin–orange juice	–	–	–	–
Thermal degradation temperature (°C)					
a_w	System	$T_{d\ onset}$	$T_{d\ peak}$	$T_{d\ endset}$	ΔH_d (J/g)
0.050	Inulin	218.61 ± 0.14	228.25 ± 2.19	244.07 ± 1.07	19.68 ± 2.96
	Inulin–orange juice	201.03 ± 1.57	220.88 ± 1.99	235.06 ± 1.23	44.63 ± 2.39
0.710	Inulin	214.07 ± 2.34	224.85 ± 2.79	224.13 ± 2.43	15.77 ± 6.20
	Inulin–orange juice	201.03 ± 4.82	220.88 ± 4.27	206.64 ± 5.41	44.63 ± 3.55

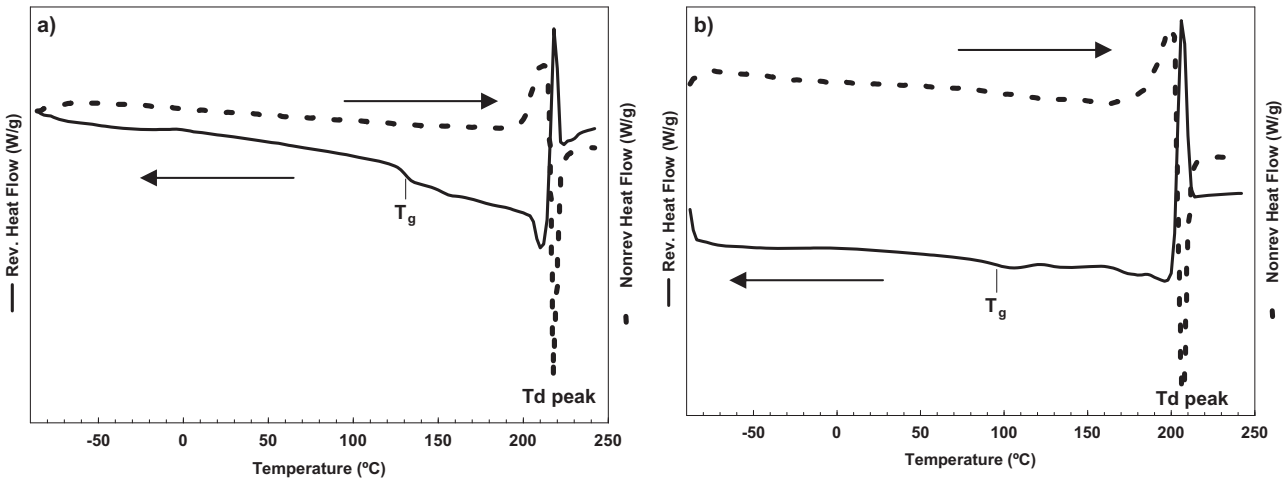

Fig. 3. Modulated DSC thermograms from systems at water activity of 0.050. (a) Inulin and (b) inulin–orange juice. Plots show the reversible heat flow on the left side of the graph (continuous line) and the non-reversible heat flow on the right side (dashed line).

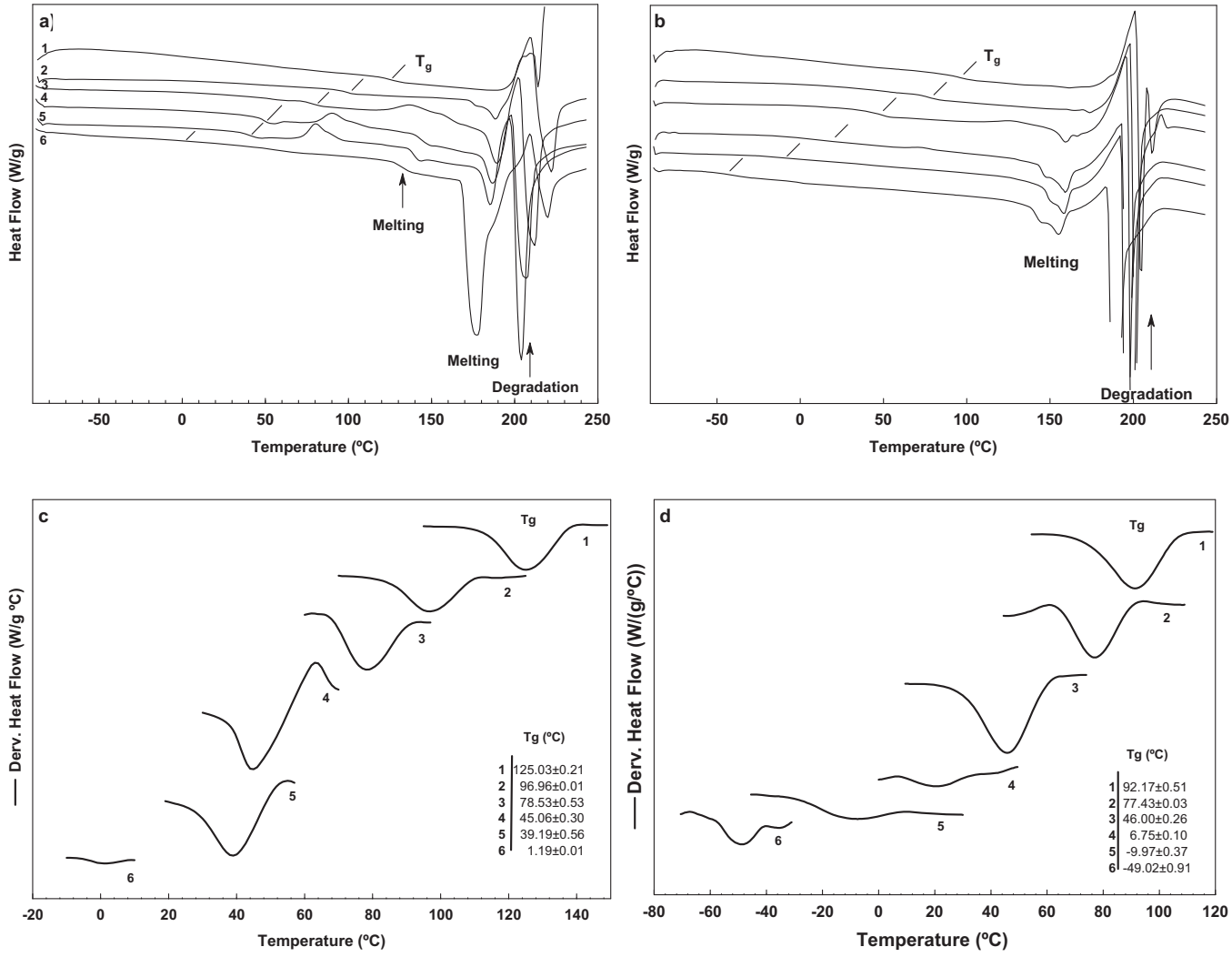

Fig. 4. Total heat flow thermograms from MDSC for systems at the different a_w: (a) and (b). First derivative of the total heat flow respect to temperature: (c) and (d). Inulin system corresponds to figures (a) and (c), while inulin–orange juice system to (b) and (d). The corresponding water activity is identified on the curves by numbers: (1) $a_w = 0.050$, (2) $a_w = 0.09$, (3) $a_w = 0.210$, (4) $a_w = 0.432$, (5) $a_w = 0.532$, and (6) $a_w = 0.710$.

and Knuutinen (2004) reported that thermal degradation occurred before melting at low heating rates (0.5–10 °C/min) and after the melting at high heating rates (20–100 °C/min). Jiang et al. (2008) observed that the caramelization degree increased with the melting time up to 110 min.

Simultaneous TGA-DSC thermal analysis showed that the inulin–orange juice system has a heterogeneous chemical composition, which is evidently caused by the low molecular weight components in the orange juice. However, a single endotherm associated with the thermal degradation was observed, regardless of the water activity. Moreover, systems as inulin and inulin–orange juice are characterized by the precise determination of their melting and degradation temperatures. Therefore, it is necessary to employ a technique that contributes to accurately separate these transitions as well as to correctly identify the glass transition temperature (T_g). This is where the results of simultaneous TGA-DSC are used for establishing an appropriate methodology for determining the T_g (Saavedra-Leos et al., 2012).

3.3. Modulated differential scanning calorimetry (MDSC)

It is noteworthy that MDSC technique allows separating both reversible and non-reversible heat flow contributions, which leads to a more accurate discrimination of the heat flow for calculating the heat capacity and determining the T_g (Verdonck, Schaap, & Thomas, 1999). The thermograms from the modulated DSC for inulin and inulin–orange juice at water activity of 0.05 are shown in Fig. 3A and B, respectively. In these figures, the reversible heat flow (W/g) is plotted on the left side of the graph, while the Non-reversible heat flow is plotted on the right side. On the reversible heat flow curves, a slight variation in the slope is observed, which corresponds to an endothermic change associated with a second order phase transition (T_g). Glass transition temperature is physically interpreted as the structural relaxation between the glassy and rubbery states. For example, T_g for inulin was observed at 126 °C, while for inulin–orange juice was observed 90 °C. On the Non-reversible heat flow curves a single event is shown corresponding to the degradation temperature identified as $T_{d\ peak}$. Thermal degradation is a kinetic process depending on temperature and time and involving a non-reversible heat flow. For inulin, degradation temperature was found at 228 °C, while for inulin–orange juice it was 220 °C; these results agree with those found from the simultaneous TGA-DSC analyses. Melting signal was not observed for any of the two systems, indicating that both systems are fully amorphous at this low water activity (Dan et al., 2009).

Fig. 4A and B shows the total heat flow plotted against the temperature for inulin and inulin–orange juice systems, at the different water activities; this heat is the sum of the reversible and non-reversible heat flows. In these figures, a slight variation in the slope of the curve is observed, which corresponds to an endothermic change associated with a second order phase transition (T_g). For example, at a water activity of 0.05, T_g for inulin was found at 126 °C while for inulin–orange juice it was 90 °C. This transition is indicated in the figure by a slash (/) for each water activity. It is clear in both systems that T_g decreases as water activity increases. These results are in accordance with those reported by Ronkart et al. (2006), Ronkart et al. (2009), and Zimeri and Kokini (2003), who observed a similar behavior for amorphous inulin and found that T_g transition (signal intensity) is more pronounced for the more amorphous systems. With the aim of observing more clearly the T_g, the first derivative of the total heat flow respect to temperature was calculated and plotted in Fig. 4C and D. In these figures, only the temperature range where transition was carried out is plotted. Evidently, T_g shifted toward lower temperature as the water activity increased from 0.05 to 0.710. Inulin presented a decrease in the T_g from 125 to 1 °C, while for inulin–orange juice T_g decreased

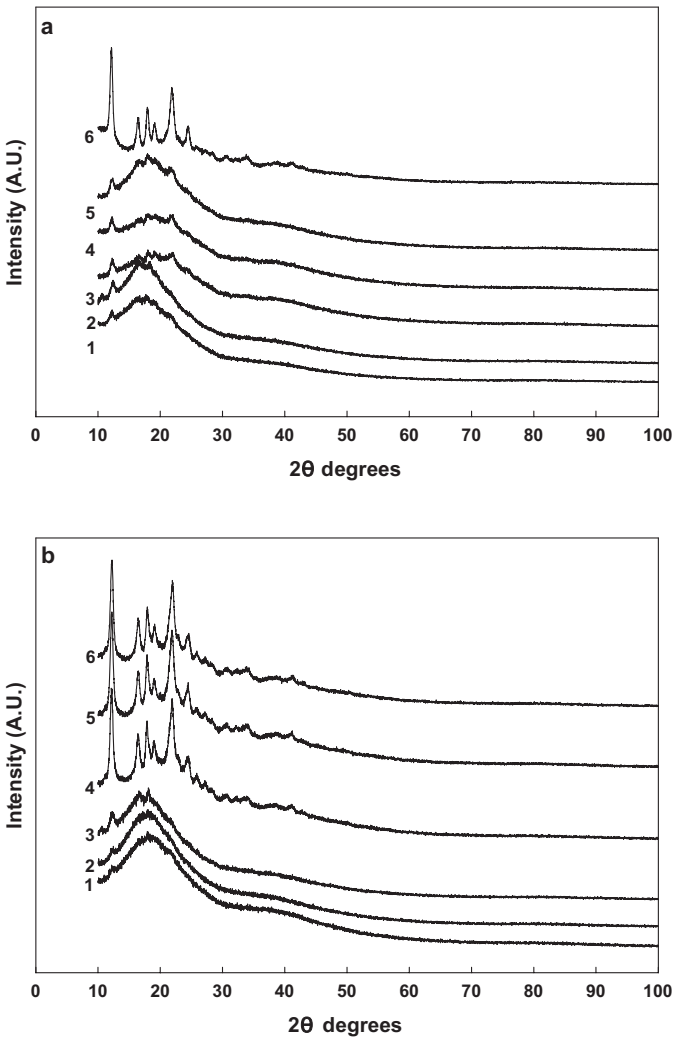

Fig. 5. X-ray diffractograms for systems at different a_w: (a) inulin and (b) inulin–orange juice. The corresponding water activity is identified on the curves by numbers: (1) a_w = 0.050, (2) a_w = 0.09, (3) a_w = 0.210, (4) a_w = 0.432, (5) a_w = 0.532, and (6) a_w = 0.710.

from 93 to −43 °C; these results are summarized. This phenomenon is explained in terms of structural disorder. When water is added, the polymeric system loses its compaction and rigidity. Thus, water molecules act a plasticizer, introducing themselves into the polymeric chains, increasing the intermolecular distance or free volume and the molecular mobility (Collares, Kieckbusch, & Finzer, 2002). Macroscopically, this is observed as a lower viscosity. Now, when comparing the T_g of both systems, the inulin–orange juice presented a lower transition temperature. This is related not only to the addition of water into the system, but also to the complex chemical composition of the orange juice. This juice is characterized by a high content of low molecular weight components as fructose, glucose and citric acid, which have a T_g ranging from 12 to 62 °C (Slade & Levine, 1994)

After T_g, the next observed events are crystallization exotherms, melting and degradation endotherms. In Fig. 4A for thermograms identified as 3, 4 and 5, an exothermic peak can be observed located at temperatures of 135, 90 and 80 °C, respectively. The peak is a second order transition associated with the crystallization of amorphous inulin. Inulin is considered a biopolymer that exhibits a similar behavior to that of a synthetic polymer. Within polymer science it is well known that when a polymer crystallizes from the melt and due to the high viscosity and low free volume, it will form

large system imperfections. Such imperfections cause the polymer chain entanglement, resulting in a less thermodynamically stable structure. In contrast, when crystallization occurs from the solution, the viscosity in the system decreases while the free volume increases; these conditions facilitate the arrangement of molecules in a more ordered and thermodynamically stable structure (Mathot, 2010). According to the above, as water adsorption increases in our systems, inulin molecules move more easily due to the variations in the viscosity and in the free volume. Thereby the system is arranged more thermodynamically stable structure, allowing the crystallization of amorphous inulin (Kedward, MacNaughtan, & Mitchell). While this argument helps to understand why inulin crystallizes, it does not explain why the crystallization temperature shifts toward lower temperatures as water adsorption increases. Ronkart et al. (2009) reported that crystallization temperature for inulin decreases with the water content. Likewise, Martin and Avérous (2001) showed a decrease in the crystallization temperature of lactic acid when using glycerol as plasticizer. Crystallization is a kinetic phenomenon dependent on temperature, where a better molecular arrangement is carried out at low heating rates. After crystallization, several melting endotherms are observed in both systems. For inulin, two well-separated endotherms are observed at temperature ranges of 125–138 and 172–193 °C. Inulin–orange juice also presented two endotherms very close to each other, separated only by the melting peak. These endotherms ranged in a temperature of 140–170 °C. The presence of several melting endotherms indicates the formation of crystals with different quality. André et al. (1996) found that inulin crystals differing in size, perfection and molecular weight showed differences in their thermal behavior. In this sense, Ronkart et al. (2009) observed a double endothermic peak at 171 and 178 °C and correlated these peaks with the melting of crystals differing in perfection. Leyva-Porras, Esneider-Alcalá, Toxquí-Terán, Márquez-Lucero, and Aguilar-Martínez (2013) found that for high density polyethylene the perfection of the crystals is related with the changes in melting temperature, where crystals smaller in size melt at lower temperature than those of bigger size.

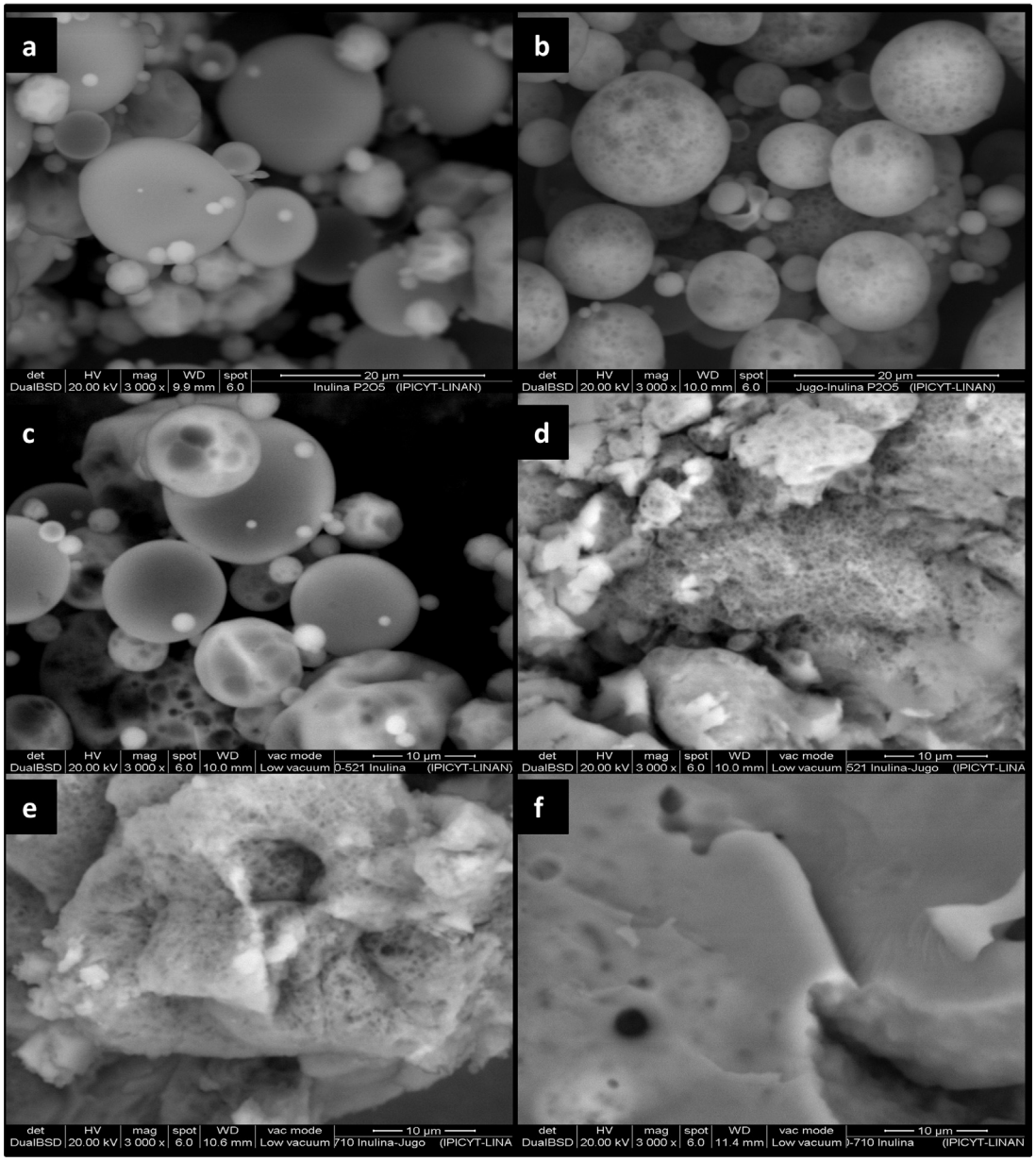

Fig. 6. SEM images from powdered samples at three water activities corresponding to $a_w = 0.050$, $a_w = 0.523$ and $a_w = 0.710$ and arranged in the figure from top to bottom, respectively. Images on the left column correspond to the inulin (a, c and d), while those on the right side correspond to inulin–orange juice system (b, d and f).

Clearly, the adsorption of water promotes crystallization of inulin, due to increased molecular mobility which induces the formation of small crystals.

Following to the melting, degradation was observed. Inulin degraded in the temperature range of 198–213 °C, while inulin–orange juice degraded in the range of 180–206 °C.

Recently, the water content and glass transition temperature have been used together for evaluating and predicting the storage stability of a product. Products having water content near the monolayer value and stored at temperatures below their T_g, have shown a relatively large stability. Ronkart et al. (2006) remarked that T_g is a good indicator for predicting the stability of products. Similarly, Telis and Martinez-Navarrete (2009) reported that a product is stable for several periods of storage when the physical state is not altered with time. Therefore, products presenting a high T_g and low water content will last more time stored in good conditions. For this reason, the determination of T_g should be carried out accurately and this is achieved employing a modulated DSC. Finally, the importance of analyzing the inulin and inulin–orange juice systems with different water contents by MDSC falls upon predicting their behavior during storage, preventing agglomeration (caking) and increasing the product shelf life.

3.4. X-ray diffraction

A great advantage of employing X-ray diffraction for characterizing dried powders relies in the amount of sample used for the analysis; this amount can be considered as more representative from sample. Fig. 5 shows the X-ray diffractograms for both systems inulin and inulin–orange juice at different water activities. At low water activities (0.05 and 0.09) a single diffraction peak over a broad diffraction band is observed. The broad band indicates the overall amorphous state. As water activity increased crystallinity was observed; the initial intensity of the diffraction

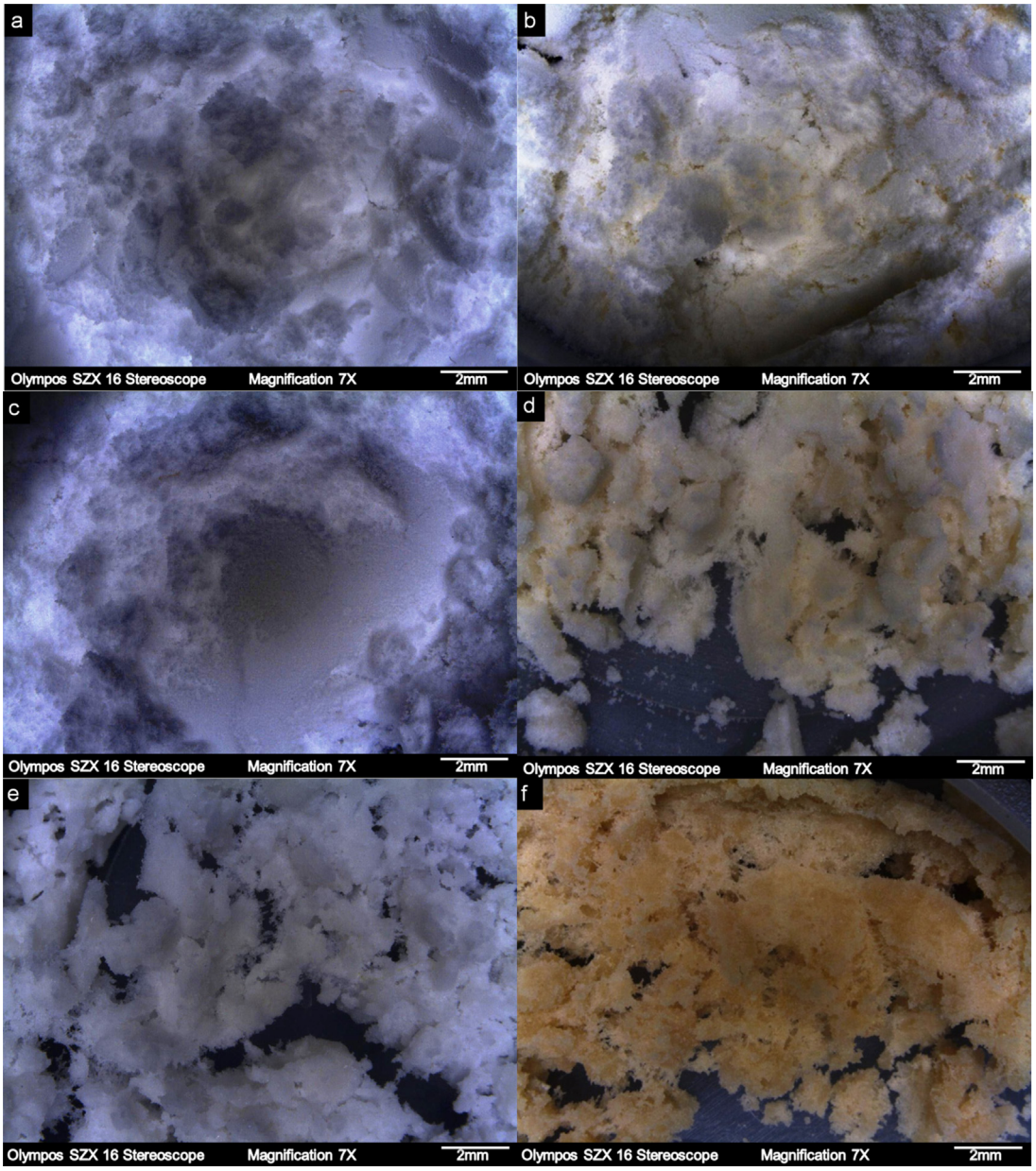

Fig. 7. Optical micrographs from powdered samples at three water activities corresponding to $a_w = 0.050$, $a_w = 0.523$ and $a_w = 0.710$ and arranged in the figure from top to bottom, respectively. Images on the left column correspond to the inulin (a, c and e), while those on the right side correspond to inulin-orange juice system (b, d and f).

peak at $2\theta = 12^{\circ}$ started to increase while more peaks developed. This behavior was also observed for inulin by Dan et al. (2009), Marchessault, Bleha, Deslandes, and Revol (2009) and Ronkart et al. (2006). Then, increasing water content produces a major molecule mobility, which favors the rearrangement of the structure, from a metastable state (amorphous) into a more thermodynamically stable state (crystalline) (André, Putaux, et al., 1996; André, Mazeau, et al., 1996). In the other hand, when comparing the two systems, inulin reached the highest crystallinity at a water activity of 0.710, while for inulin–orange juice it was at a_w of 0.437. Above this value, crystallinity remained unchanged for the system containing orange juice. As stated before, in the complex system containing orange juice, the low molecular weight components move more easily into the sample, interacting with it and contributing to reach a more stable state. Burnett et al. (2006) reported that the crystallinity degree is more affected in systems containing a large amount of low molecular weight sugars. In general, XRD results agree well with those from TGA-DSC and MDSC experiments.

3.5. Microstructure and optical appearance

At this point, through thermal analysis, MDSC and XRD we have determined quantitatively and qualitatively the effect of water content on the structure for the two systems. However, from the industrial point of view, other phenomena may be evaluated more easily. Thus, agglomeration or caking is a phenomenon, which is commonly determined visually and for this purpose we employed SEM and optical microscopy. Fig. 6 shows micrographs acquired from the SEM. Images on the left column correspond to the inulin, while those on the right side correspond to inulin–orange juice system. Three water contents (a_w) were chosen: low (0.05), medium (0.523) and high (0.710), arranged in the figure from top to bottom. At low water content, both systems presented similar morphology, where well-defined spheres are observed. These spheres are of different sizes and contain the components from inulin (Fig. 6A) and inulin–orange juice (Fig. 6B). However, spheres for inulin appear with a smooth surface, while those for inulin–orange juice show a porous surface. Evidently, this difference relies on the complexity of the inulin–orange juice system. At medium water content, inulin system showed almost the same spherical morphology, showing few zones with non-spherical material as in Fig. 6C. Unexpectedly, inulin–orange juice system showed a very different morphology at medium water content. As observed in Fig. 6D spheres are no longer appreciated and the material seems just agglomerated. At the highest water content, both systems presented the appearance of agglomerated material. Here, we can relate the microstructure observed by SEM with the results obtained from the other characterization techniques (TGA-DSC, MDSC and XRD). Clearly, at low water content the structure of the material is amorphous and this corresponds to the spherical morphology. As water content was increased, the crystalline structure was developed and morphology changed from spheres into agglomerated material. These results and observations agree with those reported by Ronkart et al. (2009) who studied stability of inulin by SEM.

Optical microscopy images are shown in Fig. 7. Images were ordered in the same fashion as in Fig. 6. The overall look of the powders resembles that of a material in bulk. Anyway, the most distinguishable feature is the change in color as the water content was increased. Initial color for inulin system was white and this remained almost unchangeable at higher water content. Unlike inulin, inulin–orange juice system showed a yellowish color at low water content and this appearance changed to an orange-like color at the highest water content. Obviously, the change in color is related with the changes in crystallinity caused by the water content and the low molecular weight species in the orange juice. Another feature observed from the images is the morphology of the particles. In both systems, at low water content material is randomly accommodated i.e. without a specific morphology. As water content increases and thus crystallinity is induced, needle shaped morphology is developed. This morphology produces an overall appearance, which can be employed for visually distinguishing a crystallized system from an amorphous one.

4. Conclusions

The effect of water content on both inulin and inulin–orange juice systems prepared by spray-drying was studied by several characterization techniques. A fully amorphous structure in both systems was reached after the spray drying process. By storing the systems under different water activities (a_w), changes in the structure and the thermal properties were observed and related to the moisture content. Moisture content was largely influenced by the chemical composition of the systems, being the inulin–orange juice more complex. Moisture adsorption was fitted by the GAB model and presented an isotherm type II. The monolayer water content was greater for the inulin–orange juice system. At low a_w, both systems presented a fully amorphous structure. As a_w increased, crystallinity was developed reaching a semicrystalline structure. Semicrystalline state was observed at low a_w for the inulin–orange juice system. This was corroborated by TGA-DSC and XRD experiments. Glass transition temperature determined by MDSC, showed a decrease with a_w. Inulin–orange juice system presented lower T_g than inulin. SEM and optical microscopy images provided a very good insight about the amorphous and crystalline microstructures developed by the systems. The present work allows establishing that structural changes in amorphous systems such are inulin and inulin–orange juice, are not caused only by the water adsorption but the chemical composition plays a major role in this process.

Acknowledgments

The technical support provided by Alberto Toxqui and Miguel Esneider, and the support of the Consejo Nacional de Ciencia y Tecnología (CONACyT) through the Postdoctoral scholarship 290679_20755, are gratefully acknowledged.

References

Abd-Elrahman, M. I., & Ahmed, S. M. (2009). Thermal degradation kinetics and geometrical stability of D-sucrose. *International Journal of Polymeric Materials*, *58*, 322–335.

Adhikari, B., Howes, T., Lecomte, D., & Bhandari, B. R. (2001). A glass transition temperature approach for the prediction of the surface stickiness of a drying droplet during spray drying. *Powder Technology*, *149*, 168–179.

André, I., Mazeau, K., Tvaroska, I., Putaux, J. L., Winter, W. T., Taravel, F. R., et al. (1996). Molecular and crystal structures of inulin from electron diffraction data. *Macromolecules*, *29*, 4626–4635.

André, I., Putaux, J. L., Chanzy, H., Taravel, F. R., Timmermans, J. W., & Wit, D. (1996). Single crystals of inulin. *International Journal of Biological Macromolecules*, *18*, 195–204.

Arthey, D., & Ashurst, P. (2001). *Fruit processing: Nutrition, products and quality management* (2nd edition, pp. 312). UK, Springer Ed.: An Aspen Publication.

Braunauer, S., Deming, L. S., Deming, W. E., & Teller, E. (1940). On a theory of the Van der Waals adsorption of gases. *Journal of the American Chemical Society*, *62*, 1723–1732.

Burnett, D. J., Thielmann, F., Sokoloski, T., & Brum, J. (2006). Investigating the moisture-induced crystallization kinetics of spray-dried lactose. *International Journal of Pharmaceutics.*, *313*, 23–28.

Chiou, D., & Langrish, T. A. G. (2007). Crystallisation of amorphous components of spray-dried powders. *Drying Technology*, *25*(9), 971–983.

Collares, F. P., Kieckbusch, T. G., & Finzer, J. R. D. (2002). Review: Glass transition in food products. *Brazilian Journal of Food Technology*, *5*, 117–130.

Dan, A., Ghosh, S., & Moulik, S. P. (2009). Physicochemical studies on the biopolymer inulin: A critical evaluation of its self-aggregation, aggregate-morphology, interaction with water. *Biopolymers*, *91*(9), 687–699.

Derycke, D. G., & Vandamme, E. J. (1984). Production and properties of *Aspergillus niger* inulinase. *Journal of Chemical and Biotechnology*, *35*, 45–51.

Farnworth, E. R., Lagacé, M., Couture, R., Yaylayan, V., & Stewart, B. (2001). Thermal processing, storage conditions and the composition and physical properties of orange juice. *Journal of Food Engineering*, *34*, 25–30.
Glibowski, P., & Pikus, S. (2011). Amorphous and crystal inulin behavior in a water environment. *Carbohydrate Polymers*, *83*, 635–639.
Goula, A. M., Karapantsios, T. D., Achilias, D. S., & Adamopoulos, K. G. (2008). Water sorption isotherms and glass transition temperature of spray dried tomato pulp. *Journal of Food Engineering*, *85*, 73–83.
Hurtta, M., Pitkänen, I., & Knuutinen, J. (2004). Melting behavior of D-sucrose, D-glucose and D-fructose. *Carbohydrate Research*, *339*, 2267–2273.
Jaya, S., & Das, H. (2009). Glass transition and sticky point temperatures and stability/mobility diagram of fruit powders. *Food and Bioprocess Technology*, *2*, 89–95.
Jiang, B., Liu, Y., Bhandari, B., & Zhou, W. (2008). Impact of caramelization on the glass transition temperature of several caramelized sugars. Part I: Chemical analyses. *Journal of Agricultural and Food Chemistry*, *56*, 5138–5147.
Kawai, K., Fukami, K., Thanatuksorn, P., Viriyarattanasak, C., & Kajiwara, K. (2011). Effects of moisture content, molecular weight, and crystallinity on the glass transition temperature of inulin. *Carbohydrate Polymers*, *83*, 934–939.
Kedward, C. J., MacNaughtan, W., & Mitchell, J. R. (2000). Crystallization kinetics of amorphous lactose as a function of moisture content using isothermal differential scanning calorimetry. *Journal of Food Science*, *65*, 324–328.
Khalloufi, S., El-Maslouhi, Y., & Ratti, C. (2000). Mathematical model for prediction of glass transition temperature of fruit powders. *Journal of Food Science*, *65*(5), 842–848.
Kiranoudis, C. T., Maroulis, Z. B., Tsami, E., & Marinos-Kouris, D. (1993). Equilibrium moisture content and heat of desorption of some vegetables. *Journal of Food Engineering*, *20*, 55–74.
Labuza, T. P., & Hyman, C. R. (1998). Moisture migration and control in multi-domain foods. *Trends in Food Science and Technology*, *9*, 47–55.
Lee, J. W., Thomas, L. C., & Schmidt, S. J. (2011). Can the thermodynamic melting temperature of sucrose, glucose and fructose be measured using rapid-scanning differential scanning calorimetry (DSC). *Journal of Agricultural and Food Chemistry*, *59*, 3306–3310.
Lewicki, P. P. (1997). The applicability of the GAB model to food water sorption isotherms. *J. Food Sci. Technol.*, *32*, 553–557.
Leyva-Porras, C., Esneider-Alcalá, M., Toxquí-Terán, A., Márquez-Lucero, A., & Aguilar-Martínez, J. (2013). Effect of molding parameters on Young's modulus of an injected molded low-density polyethylene (LDPE). *Industrial & Engineering Chemistry Research*, *52*, 5666–5671.
Marchessault, R. H., Bleha, T., Deslandes, Y., & Revol, J. F. (1980). Conformation and crystalline of (2-1) β-D-fructofuranan (inulin). *Canadian Journal of Chemistry*, *58*, 2415–2422.
Martin, O., & Avérous, L. (2001). Poly(lactic acid): Plasticization and properties of biodegradable multiphase systems. *Polymer*, *42*, 6209–6219.
Mathot, V. B. F. (2010). Crystallization of polymers. *Journal of Thermal Analysis and Calorimetry*, *102*, 403–412.
Orsi, F. (1973). Kinetic studies on the thermal decomposition of glucose and fructose. *Journal of Thermal Analysis*, *5*, 329–335.
Pitarresi, G., Giacomazza, D., Triolo, D., Giammona, G., & Biagio, P. L. S. (2012). Rheological characterization and release properties of inulin-based hydrogels. *Carbohydrate Polymers*, *88*, 1033–1040.
Rhaman, M. S. (2010). Food stability determination by macro-micro region concept in the state diagram and by defining a critical temperature. *Journal of Food Engineering*, *99*(4), 402–416.
Ronkart, N. S., Blecker, C., Fougnies, C., Van Herck, J. C., Wouters, J., & Paquot, M. (2006). Determination of physical changes of inulin related to sorption isotherms: An X-ray diffraction, modulated differential scanning calorimetry and environmental scanning electron microscopy study. *Carbohydrate Polymers*, *63*, 210–217.
Ronkart, N. S., Paquot, M., Fougnies, C., Deroanne, C., & Blecker, C. (2009). Effect of water uptake on amorphous inulin properties. *Food Hydrocolloids*, *23*, 922–927.
Roos, Y. H. (1995). *Phase transition in foods*. San Diego, CA, USA: Academic Press, Food Science and Technology.
Roos, Y. H. (2002). Importance of glass transition and water activity to spray drying and stability of dairy powders. *Lait*, *82*, 475–484.
Saavedra-Leos, M. Z., Álvarez-Salas, C., Esneider-Acala, M. A., Toxqui-Terán, A., Pérez-García, S. A., & Ruiz-Cabrera, M. A. (2012). Towards an improved calorimetric methodology for glass transition temperature determination in amorphous sugars. *Journal of Food*, *10*(4), 258–267.
Sablani, S. S., Kasapis, S., & Rahman, M. S. (2007). Evaluating water activity and glass transition concepts for food stability. *Journal of Food Engineering*, *78*, 266–271.
Sablani, S. S., Syamaladevi, R. M., & Swanson, B. G. (2010). A review of methods, data and applications of state diagrams of food systems. *Food Engineering Reviews*, *2*, 168–203.
Slade, L., & Levine, H. (1988). Non-equilibrium behavior of small carbohydrate–water systems. *Pure and Applied Chemistry*, *60*(12), 1841–1864.
Slade, L., & Levine, H. (1994). Water and the glass transition-dependence of the glass transition on composition and chemical structure: Special implications for flour functionality in cookie baking. *Journal of Food Engineering*, *22*, 143–188.
Telis, V. R. N., & Martinez-Navarrete, N. (2009). Collapse and color changes in grapefruit juice powder as affected by water activity, glass transition, and addition of carbohydrate polymers. *Food Biophysics*, *4*, 83–93.
Vanhal, I., & Blond, G. J. (1999). Impact of melting conditions of sucrose on its glass transition temperature. *Journal of Agriculture and Food Chemistry*, *47*, 4285–4290.
Verdonck, E., Schaap, K., & Thomas, L. C. (1999). A discussion of the principles and applications of modulated temperature DSC (MTDSC). *International Journal of Pharmaceutics*, *192*, 3–20.
Zimeri, J. E., & Kokini, J. L. (2003). Phase transitions of inulin–waxy maize starch systems in limited moisture environments. *Carbohydrate Polymers*, *51*, 183–190.